Iris Extraction Based on Intensity Gradient and Texture Difference

Guodong Guo
Dept. of Computer Science
North Carolina Central University
gdguo@nccu.edu

Michael J. Jones
Mitsubishi Electric Research Laboratories
mjones@merl.com

Abstract

Biometrics has become more and more important in security applications. In comparison with many other biometric features, iris recognition has very high recognition accuracy. Successful iris recognition depends largely on correct iris localization, however, the performance of current techniques for iris localization still leaves room for improvement. To improve the iris localization performance, we propose a novel method that optimally utilizes both the intensity gradient and texture difference. Experimental results demonstrate that our new approach gives much better results than previous approaches. In order to make the iris boundary more accurate, we present a new issue called model selection and propose a method to choose between ellipse/circle and circle/circle models. Furthermore, we propose a dome model to compute mask images and remove eyelid occlusions in the unwrapped images rather than in the original eye images with a least commitment strategy.

1. Introduction

A wide variety of systems require reliable personal identification or verification. Biometric technology overcomes many of the disadvantages of conventional identification and verification techniques such as keys, ID cards and passwords. Biometrics refers to the automatic recognition of individuals based on their physiological and/or behavioral characteristics [12]. There are many features to use as biometric cues, such as face, fingerprint, hand geometry, handwriting, iris, retinal vein, and voice. Among all these features, iris recognition has very high accuracy [17]. The complex iris texture carries very distinctive information. Even the irises of identical twins are different [7] [12].

For a captured iris image, the iris analysis begins with iris localization. There are two fundamental approaches to localize the iris in eye images. One is Daugman's integro-differential operator (IDO) [8], and the other is the Hough transform technique [22]. Later on, some other approaches are proposed that are essentially minor variations of the two classical methods.

Daugman [8] presented the first approach to computational iris recognition including iris localization. He proposed to use an integro-differential operator (IDO) for locating the inner and outer boundaries of an iris via the following optimization,

$$\max_{(r,x_0,y_0)} \left| G_\sigma(r) * \frac{\partial}{\partial r} \oint_{r,x_0,y_0} \frac{I(x,y)}{2\pi r} ds \right| \qquad (1)$$

where $I(x,y)$ is an image containing an eye. The IDO searches over the image domain (x,y) for the maximum in the blurred partial derivative with respect to increasing radius r, of the normalized contour integral of $I(x,y)$ along a circular arc ds of radius r and center coordinates (x_0, y_0). The symbol $*$ denotes convolution and $G_\sigma(r)$ is a smoothing function such as a Gaussian of scale σ.

Daugman's IDO actually behaves as a circular edge detector. The IDO searches the gradient maximum over the 3D parameter space, so there is no need to use any threshold as in the traditional Canny edge detector [4].

Later, Wildes [22] proposed to detect edges in iris images followed by circular Hough transform [11] to localize iris boundaries. The Hough transform searches the optimum parameters of the following,

$$\max_{(r,x_0,y_0)} \sum_{j=1}^{n} h(x_j, y_j, x_0, y_0, r) \qquad (2)$$

where

$$h(x_j, y_j, x_0, y_0, r) = \begin{cases} 1, & if \;\; g(x_j, y_j, x_0, y_0, r) = 0 \\ 0, & otherwise \end{cases}$$

with $g(x_j, y_j, x_0, y_0, r) = (x_j - x_0)^2 + (y_j - y_0)^2 - r^2$ for edge point $(x_j, y_j), j = 1, \cdots, n$.

One weak point of the edge detection and Hough transform approach is the use of thresholds in edge detection. Different settings of threshold values may result in different edges and then affect the Hough transform results significantly [20].

Recently, some other methods have been proposed for iris localization. But most of them are essentially minor variants of Daugman's IDO or Wildes' combination of edge detection and Hough transform, by either constraining the parameter search range or speeding up the search process. For example, Ma *et al* [15] roughly estimates the pupil position through pixel intensity value projections and thresholding, and then do Canny edge detection and circular Hough transform. Masek [18] implemented an edge detection method slightly different from the Canny [4], and then used circular Hough transform for iris boundary extraction. He also made his Matlab code public available. Cui et al [6] computed a wavelet transform and then used the Hough transform to locate the iris inner boundary, while using Daugman's IDO for the outer boundary. Rad *et al* [21] used gradient vector pairs at various directions to coarsely estimate positions of the circle and then used Daugman's IDO to refine the iris boundaries. Kim *et al* [13] used mixtures of three Gaussian distributions to coarsely segment eye images into dark, intermediate, and bright, and then use the Hough transform for iris localization. Liu *et al* [14] used some heuristics to improve the Hough transform results including the reduction of edges and the modification of the Hough voting. A level set method was used in [2].

1.1. Motivation of Our Work

A common observation on eye images is that the iris region is brighter than the pupil and darker than the sclera. As a result, almost all previous approaches to iris localization are based on the intensity gradient or edge information. These methods depend heavily on the strong intensity contrast between pupil and iris and between iris and sclera. However, these contrasts are not always strong enough for iris localization in practice.

Our new observation is that the iris region has very different structure or texture from that of the pupil and sclera. We believe that this texture difference is also useful for discrimination between iris and pupil or between iris and sclera, especially when the intensity contrast is not strong enough for iris localization. In fact, the rich texture information in the iris is used for iris recognition.

Based on this new observation, we develop a new technique that combines the texture difference between iris and sclera or between iris and pupil together with the intensity contrast. The purpose is to improve the iris localization performance significantly.

The remainder of the paper is organized as follows. In Section 2 a new approach to iris localization is presented. We discuss a new issue called model selection and give a solution in Section 3. The mask image computation is presented in Section 4. The experiments are shown in Section 5, and finally some conclusions are given.

2. Intensity Gradient and Texture Difference

As discussed in previous Section, our approach to iris localization is to use both the intensity gradient and texture difference. The new formulation for iris localization is the following optimization,

$$\begin{aligned}(r^*, x_0^*, y_0^*) &= \arg\max_{(r,x_0,y_0)} C(I, x_0, y_0, r) \\ &+ \lambda\, T(Z_i, Z_o, x_0, y_0, r)\end{aligned} \quad (3)$$

where $C(I, x_0, y_0, r)$ is the intensity contrast or gradient over image domain $I(x, y)$ along a circle (x_0, y_0, r), and $T(Z_i, Z_o, x_0, y_0, r)$ measures the texture difference between the inner zone Z_i and outer zone Z_o separated by the circular boundary (x_0, y_0, r), as shown in Fig. 1. The parameter λ is a constant to balance the contributions from intensity gradient and texture difference. Since the whole region inside or outside the circle is not necessarily uniform or homogeneous, e.g., the inner region of the iris/sclera boundary contains two different parts, pupil and iris, thus only a narrow zone next to the circular boundary is used to measure the texture property.

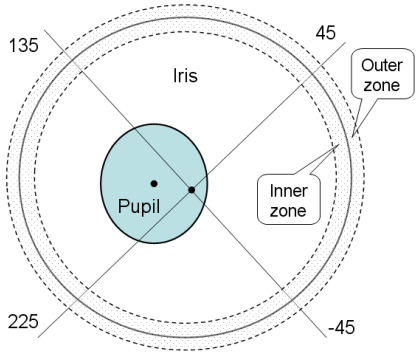

Figure 1. Show the inner and outer zones separated by a circle (solid line between two dashed lines) for iris/sclera boundary. The texture difference are measured between the inner and outer zones in addition to the intensity gradient for iris localization. Because of possible eyelid occlusion, the search is restricted to the left and right quadrants, i.e, -45 to 45 and 135 to 225 degrees. This figure also illustrates that the pupil and iris may not be concentric and the pupil/iris boundary may be modeled by an ellipse instead of a circle.

What is the specific form for each term in Eq. (3)? For the first term, i.e, intensity gradient or contrast, we choose to use Daugman's integro-differential operator, because the IDO can encode the image intensity gradient very well along a circular boundary. Thus we have

$$C(I, x_0, y_0, r) = \left| G_\sigma(r) * \frac{\partial}{\partial r} \oint_{r,x_0,y_0} \frac{I(x, y)}{2\pi r} ds \right| \quad (4)$$

For the second term in Eq. (3), we use the Kullback-Leibler divergence (See Section 2.2) to measure the distance

between two probability distributions derived from the inner and outer zones, respectively. Now the question is how to extract the texture information from each zone. One may think of using the standard texture analysis method, e.g, Gabor filters. But the problem is that the filtering approach usually needs a large region support which may go across the circular boundary. This is a general issue in texture segmentation where the regional property may be characterized well but the boundary between two textures can not be located precisely. For iris localization, it really needs accurate boundaries to normalize and match iris images. Inaccurate iris localization deteriorates the iris recognition accuracy quickly no matter how discriminative the iris feature is.

To efficiently extract the texture properties without influencing the iris localization negatively, we use a method called local binary pattern (LBP) with the smallest neighborhood.

2.1. Local Binary Pattern

The local binary pattern (LBP) operator is a simple yet powerful method of analyzing textures [16]. It was first proposed by Ojala *et al* [19] for texture classification. The basic operation of LBP consists of three steps as shown in Fig. 2 using a 4-neighbor system: (1) thresholding the pixel values of all neighbors using the intensity value of the center pixel as the threshold, (2) weighting each neighbor with a value associated with the power of 2, and (3) summing up new values of all neighbors and setting it for the center pixel.

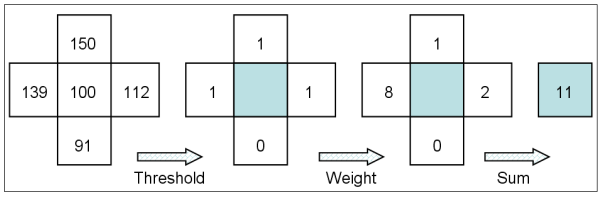

Figure 2. Illustrate the LBP operator in a 4-neighbor case. Threshold the 4 neighbors with respect to the center pixel, weight each neighbor with a different number of the power of 2, and finally summ up the new integers to get a new value for the center pixel. This process is executed for each pixel under consideration.

The pixels in a region of interest are encoded by new integers with the LBP operator. Then the histogram of these new integers for each zone is computed to represent its probability density function. In our case, a 4-neighbor system is considered for the LPB operator, the resulting new integer value for each center pixel is between 0 and 15, so each histogram has 16 bins. The LBP operator is executed for the whole image just once, while the histogram is computed dynamically in the search process.

The probability densities are computed for the inner and outer zones respectively, denoted as $p(x; Z_i)$ and $q(x; Z_o)$, or simply $p(x)$ and $q(x)$ without confusion, where $x \in \{0, \cdots, 15\}$. The distance between two probability distributions is measured by the following KL-divergence.

2.2. KL-Divergence

Given two probability mass function $p(x)$ and $q(x)$, the Kullback-Leibler divergence (or relative entropy) between p and q is defined as

$$D(p||q) = \sum_x p(x) \log \frac{p(x)}{q(x)} \tag{5}$$

The KL-divergence $D(p||q)$ is always non-negative and is zero if and only if $p = q$. Even though it is not a true distance between distributions because it is not symmetric and does not satisfy the triangle inequality, it is still often useful to think of the KL-divergence as a "distance" between distributions [5].

As a result, the second term in Eq. (3) can be computed by the KL-divergence as

$$T(Z_i, Z_o, x_0, y_0, r) = D\left(p(x; Z_i)||q(x; Z_o)\right) \tag{6}$$

where Z_i and Z_o are the inner and outer zones separated with the circle (x_0, y_0, r). The probability densities $p(x; Z_i)$ and $q(x; Z_o)$ are represented by the histogram of the integers (from 0 to 15) computed by the LBP operator.

2.3. Multi-Resolution Search

The optimization in Eq. (3) is a search process. In order to reduce the search space and hence speed up the process, and also to eliminate the local maxima, we use a multi-resolution technique. The original image is smoothed and down-sampled into a much smaller image and the optimum is found there. Then the search starts again in a finer image with the initial values set by the result obtained in previous coarser resolution. The process repeats until reaching the finest image. Note that the search in each resolution is restricted to the left and right quadrants because of possible eyelid occlusions [7] as shown in Fig. 1.

3. Model Selection

Most approaches to iris localization use two circles to model the inner and outer boundaries of the iris. Using circles is simple to compute but may not fit the iris inner boundary well. Camus and Wildes [3] used an ellipse to model the pupil/iris boundary and a circle to model the iris/sclera boundary. The ellipse model fits the inner boundary better than the circle whenever the boundary is not a true circle, but the problem is, the search will be in a 4D space instead of 3D. To search in a higher dimensional space will be slower and may be error prone.

What models should be used for iris boundaries? Should the inner/outer boundaries be modeled by circle/circle or ellipse/circle[1]? We call this the model selection problem. And we believe that model selection should be data-driven rather than assigned before hand.

Our scheme is a two-step approach. First, the circle/circle model is used to approximate the inner/outer iris boundaries. Second, within the region slightly bigger than the inner circle, do the following: (1) detect edges using the Canny edge detector [4], (2) generate chain codes for the detected edge points using 8-connectivity [10], (3) choose the longest contour from all generated chains to eliminate outliers of edge points, (4) fit an ellipse for the chosen contour using a direct ellipse-fitting method [9], (5) compute the eccentricity e of the fitted ellipse, and (6) decide whether to use ellipse or circle to model the inner iris boundary with the criterion that, if $e > e_T$, choose the ellipse, otherwise, keep the circle.

Theoretically, the ellipse model also fits a circular shape. Why do we choose between ellipse and circle? The reason is that the circle model makes it simple to unwrap the iris image into a rectangular image.

The eccentricity is computed by $e \equiv \sqrt{1 - \frac{b^2}{a^2}}$ for a standard ellipse $\frac{(x-x_0)^2}{a^2} + \frac{(y-y_0)^2}{b^2} = 1$. Theoretically the eccentricity satisfies $0 \leq e < 1$ and with $e = 0$ in the case of a circle. Note that the standard ellipse has the major and minor axes consistent with the x and y axes, while the fitted ellipses in iris images may be rotated by an angle. The direct ellipse-fitting method [9] solves a generalized eigenvalue system to estimate the ellipse parameters. It does not involve any iterative computation and thus is very fast.

To show the necessity of ellipse fitting for real iris images, Fig. 3 gives an example for iris image 105_1_1 from the CASIA iris database [1] localized by different methods. The results in the left and middle images are obtained with the circle model for the inner boundary using Hough transform and the IDO respectively. It is obvious that the circle cannot fit the pupil/iris boundary well. The result in the right image uses direct ellipse fitting and the boundary is fitted precisely.

4. Mask Computation

The iris is possibly occluded by the upper and/or lower eyelids. In the earlier work [8], Daugman excluded the top and bottom part of an iris for iris feature extraction and recognition. But this may lose some useful information when very little or no eyelid occlusion exists. As argued by Wildes [22], explicit modeling of the eyelids should allow for better use of available information than simply omitting the top and bottom of the iris. In [7], Daugman used arcuate curves with spline fitting to explicitly search the eyelid boundaries. Cui *et al* [6] used a parabolic model for the eyelids and fit them separately. The upper eyelid is searched within the eyelash region, while the lower eyelid is searched from the detected edge points. Masek used straight lines to approximate the eyelids in his Matlab code [18], which usually obtains a much larger mask than necessary.

Almost all previous work explicitly estimates the eyelid boundaries in the original eye images. That is intuitive but has some problems in practice: (1) the search range for eyelids is usually large making the process slow, and (2) most importantly, the extracted eyelids are always estimated even when they do not occlude the iris.

To address these issues, we propose to compute the eyelid occlusion in the unwrapped rectangular image rather than in the original eye image. The eyelid region seems like a dome in the unwrapped image, as shown in Fig. 4 (b) and (c), so we call it a dome model.

4.1. Dome Model

There are three possible cases for the domes in the unwrapped image as shown in Fig. 4: (a) no dome, where there is no eyelid occlusion, (b) one dome, where only the upper or lower eyelid occludes, and (c) two domes, where both upper and lower eyelids occlude the iris.

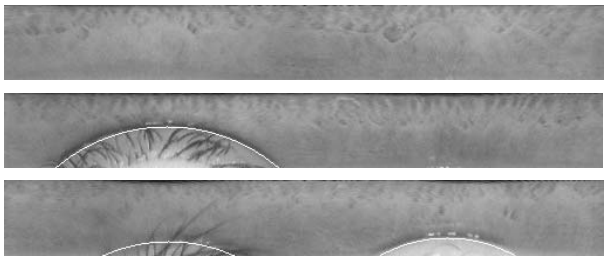

Figure 4. The dome model. There are three possible cases in an unwrapped image: (a) none dome (088_1_1), (b) only one dome (001_1_1), and (c) two domes (087_2_4). The dome boundaries are drawn with white line.

Using the new dome model, occlusions from either the upper and lower eyelids can be processed in a unified way. To extract the domes, a circle model is used to approximate instead of complex models such as splines [7] and parabolic models [6], or a rough model of straight lines [18].

Our approach to mask computation is unique in that it is a least commitment strategy. The algorithm first determines whether eyelid occlusions exist or not. If no occlusion such as in Fig. 4 (a), there is no need to call the dome search process. When occlusions do exist, the algorithm determines how many domes (1 or 2) to search, and then finds the related domes. The algorithm also has a post-processing stage to reduce possible false alarms.

[1] We do not consider an ellipse/ellipse model in that the circle usually fits the visible portion of the outer boundary well.

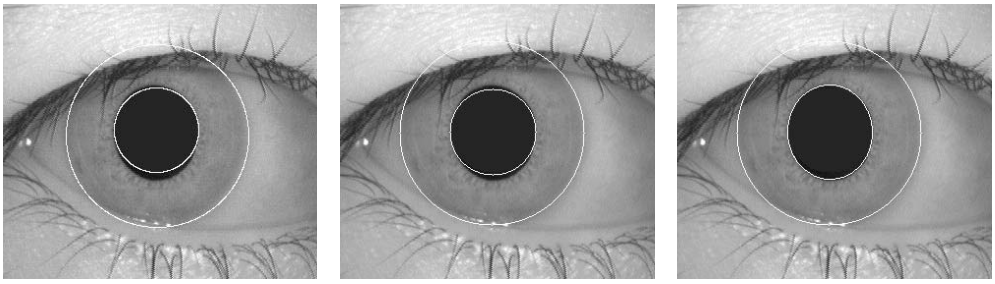

Figure 3. Demonstrate that the circle model is not accurate for the iris inner boundary. The iris image (105_1_1) uses a circle model to fit by Hough transform (left) and integro-differential operator (middle). The right image shows the result based on direct ellipse fitting. All circles and ellipse are drawn with one pixel wide white line.

To detect possible eyelid occlusions in the unwrapped image, the region of the iris where an eyelid might appear is compared to a region where occlusion cannot occur. These regions are compared by looking at their respective distributions of raw pixel values. The KL-divergence (Eqn. (5)) is used to compare the histograms of raw pixel values in the two regions.

5. Experiments

To evaluate our proposed methods for iris extraction, we use the CASIA iris database [1] that contains 756 iris images of 108 classes. For all iris images shown in this paper, original image names are also given for references.

First, we evaluate the iris localization or detection rate. In Eq. (3), λ was set to 0.1 to balance the intensity gradient and texture difference between the inner and outer zones. Actually the values of λ can range from 0.01 to 0.5 without too much influence on the performance. We simply choose a single value and keep if in all our experiments. The pixel values are normalized into $(0, 1)$ in gradient computation. In Eq. (4), the central difference approximation is used for gradient estimation with two pixel intervals. To measure the texture information with LBP operator, a 4-neighbor system was used for each pixel. This smallest neighborhood helps the boundary localization precision. The inner and outer zones are both 4-pixel wide along the radial direction that contains enough information for the structure estimation and has small computation load. The KL-divergence is computed only for bins x with $p(x) \cdot q(x) \neq 0$. The iris localization results are shown in Table 1. Our new method combining intensity gradient and texture difference can locate 97.6% irises correctly on the CASIA database, which is much better than the Hough transform technique of 85.6% and Daugman's integro-differential operator that uses only the intensity gradient of 88% iris localization rate. The correctness of the iris boundaries were determined by manual inspection.

Some examples are shown in Fig. 5 to see the localization results obtained from different methods. The upper row

Table 1. Comparison of iris detection rates on the CASIA database.

Hough Trans.	Integro-differential Oper.	Ours
85.6%	88%	97.6%

in Fig. 5 shows the results for image 037_2_4. The intensity contrast between the iris and sclera is not strong, the detected edges are weak, so the Hough transform (left image) can not find the true boundary. The IDO method (middle) gets weak gradient information especially in the left part of the iris, so the detected circle is shifted away from the true boundary. In contrast, our new method using both gradient and texture difference can deal with the case of weak gradient and gives an accurate boundary for the iris (right image, upper row). Similar analysis holds for the lower row in Fig. 5 for image 039_2_1.

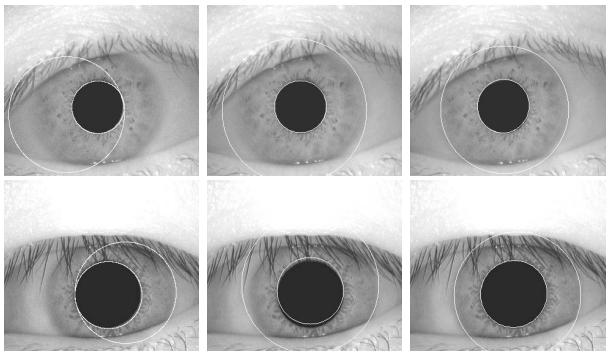

Figure 5. Comparison between different techniques for iris boundary extraction. From left to right, the results are based on Hough transform, integrodifferential operator, and the proposed new method. From top to bottom, the iris images are 037_2_4 (first row) and 039_2_1 (second row).

Second, we verify the model selection problem. Because the camera viewing line is not perpendicular to the eye, the perspective effect makes the projection of the pupil not a circle in the image plane. In addition, eyes can move freely to a certain range. As a result, the ellipse/circle model is better than the circle/circle for iris localization in some cases.

We found that there are 75.7% (572/756) iris images with eccentricity $e > 0.19$ where 0.19 is the threshold value chosen to determine whether to use ellipse/circle model or not. Our approach is to first use the circle/circle model to search the iris boundaries, and then do direct ellipse fitting for the inner boundary without turning to a 4D search. As shown in Fig. 3, for image 105_1_1, either the Hough transform (left) or IDO (middle) cannot fit well when the circle model is used for the inner boundary. On the contrary, the ellipse fitting (right) gives a much better result for the pupil/iris boundary.

Third, we evaluate the new mask computation method. As discussed in Section 4, the mask image is computed in the unwrapped images instead of the original eye images. The unwrapped image is of size 512×64 (see [8] [15] for details on how to unwrap the iris images). Our approach first determines whether there is any eyelid occlusion in the unwrapped image. If not, the algorithm does not extract any mask. Three regions are obtained with 40 by 20 pixels, starting from the image bottom. The middle region R_m is centered at 256, representing part of the iris that is never occluded by the eyelids. The left region R_l is centered at 128, and the right one R_r is at 384. Their histograms, H_l, H_m, and H_r, are computed using 32 bins.

In the CASIA iris database, our method can extract the domes with an accuracy of 93%. We found that almost all domes are detected, but the dome boundaries are not accurate for 7% (53/756) of the iris images.

6. Conclusions

We have presented a novel method for iris localization which utilizes both the intensity gradient and texture difference between the iris and sclera or between the pupil and iris. The iris localization rate based on the new method is much higher than the popular Hough transform technique and the classical integro-differential operator in that previous methods only use the gradient information and hence cannot work well when the gradient is not strong enough. Secondly, we considered the model selection problem and proposed a solution based on direct ellipse fitting. Thirdly, we presented a novel approach to mask computation in the unwrapped image. The new procedure follows a least commitment strategy that triggers the dome detection process only when necessary.

References

[1] Casia iris image database, http://www.sinobiometrics.com, 2004.

[2] E. Arvacheh and R. Tizhoosh. Iris segmentation: detecting pupil, limbus and eyelids. In *ICIP*, pages 2453–2456, 2006.

[3] T. Camus and R. Wildes. Reliable and fast eye finding in close-up images. In *Inter. Conf. on Pattern Recognition*, pages 389–394, 2002.

[4] J. Canny. A computational approach to edge detection. *IEEE Trans. on Pat. Ana. and Mach. Intel.*, 8:679–698, 1986.

[5] T. M. Cover and J. A. Thomas. *Elements of Information Theory*. Wiley, 1991.

[6] J. Cui, Y. Wang, T. Tan, L. Ma, and Z. Sun. A fast and robust iris localization method based on texture segmentation. In *Proc. SPIE on Biometric Technology for Human Identification*, volume 5404, pages 401–408, 2004.

[7] J. Daugman. How iris recognition works. *IEEE Trans. on Circuits and Systems for Video Technology*, 14:21–30, 2004.

[8] J. G. Daugman. High confidence visual recognition of persons by a test of statistical indenpendence. In *IEEE Trans. on Pat. Ana. and Mach. Intel.*, volume 15, pages 1148–1161, 1993.

[9] A. Fitzgibbon, M. Pilu, and R. Fisher. Direct least-square fitting of ellipses. *IEEE Trans. on Pat. Ana. and Mach. Intel.*, 21:476–480, 1999.

[10] R. C. Gonzalez and P. Wintz. *Digital Image Processing*. Addison-Wesley, 2rd edition, 1987.

[11] P. V. C. Hough. Method and means for recognizing complex patterns. *U.S. Patent 3 069 654*, 1962.

[12] A. K. Jain, A. Ross, and S. Prabhakar. An introduction to biometric recognition. *IEEE Trans. on Circuits and Systems for Video Technology*, 14:4–20, 2004.

[13] J. Kim, S. Cho, and J. Choi. Iris recognition using wavelet features. *Journal of VLSI Signal Processing*, 38:147–156, 2004.

[14] X. Liu, K. W. Bowyer, and P. J. Flynn. Experiments with an improved iris segmentation algorithm. In *IEEE Workshop on Auto. Ident. Adv. Technologies*, pages 118–123, 2005.

[15] L. Ma, T. Tan, Y. Wang, and D. Zhang. Personal identification based on iris texture analysis. In *IEEE Trans. on Pattern Analysis and Machine Intelligence*, volume 25, pages 1519–1533, 2003.

[16] T. Maenpaa and M. Pietikainen. Texture analysis with local binary patterns. In C. Chen and P. Wang, editors, *Handbook of Pattern Recognition and Computer Vision*, 3rd ed, pages 197–216. World Scientific, 2005.

[17] T. Mansfield, G. Kelly, D. Chandler, and J. Kane. Biometric product testing final report. *UK Biometric Work Group Report*, 2001.

[18] L. Masek and P. Kovesi. *MATLAB Source Code for a Biometric Identification System Based on Iris Patterns*. The School of Computer Science and Software Engineering, The University of Western Australia, 2003.

[19] T. Ojala, M. Pietikinen, and D. Harwood. A comparative study of texure measures with classification based on feature distributions. *Pattern Recognition*, 29:51–59, 1996.

[20] H. Proenca and L. Alexandre. Ubiris: A noisy iris image database. In *Intern. Confer. on Image Ana. and Proc.*, 2005.

[21] A. Rad, R. Safabakhsh, N. Qaragozlou, and M. Zaheri. Fast iris and pupil localization and eyhelid removal using gradient vector pairs and certainty factors. In *The Irish Machine Vision and Image Processing Conf.*, pages 82–91, 2004.

[22] R. Wildes. Iris recognition: An emerging biometric technology. *Proc. IEEE*, 85:1348–1363, 1997.